Automated Cloud Detection of Satellite Imagery Using Spatial Modeler Language and ERDAS Macro Language

Teerawong Laosuwan, Singthong Pattanasethanon and Worawat Sa-ngiamvibool

Department of Electrical and Computer Engineering, Faculty of Engineering, Mahasarakham University, Maha Sarakham 44150, Thailand

Abstract

Cloud detection from satellite imagery has been an important method of observing cloud covered areas. Presently, there are several algorithms for cloud detection, but there is no existing integrating frame and tools. The author used the software development tools within the commercial software ERDAS Imagine. The integrated software tools were the Imagine Developers' Toolkit and the C programming language. ERDAS Imagine includes its own Graphical User Interface scripting language known as ERDAS Macro Language, and its own modeling language, known as Spatial Modeling Language. The novel module of software tools can convert raster data to brightness temperature and includes a special set time function, cloud top height, and cloud cover area. This study demonstrates successful cloud detection and classification from the Multi-functional Transport Satellite-2, which will be useful in Thailand's efforts to forecast flood risks and provide early warnings of rain-causing clouds.

Keywords

Automated cloud detection, Satellite imagery, Spatial modeler language, Erdas macro language.

1. Introduction

Cloud detection from satellite data has a number of important applications in weather studies. Cloud-free pixels must be identified before the retrieval of the atmospheric and surface variables (e.g., land surface temperature and vegetation index). To accomplish high value spatial and temporal surface solar radiation, the cloud detection is indispensable to be carried out [1-4]. The cloud-free portion of an image can provide useful information about cloud size, shape, texture, and context, while images in the infrared region can inform about the water content and surface temperature. The active microwave images can be used to identify cloud structure and water content. The results of the classification are normally displayed as cloud type maps including the thin and transparent high clouds (cirrus family), thick and opaque middle and low clouds (cumulus family in particular), and the huge vertically developing clouds (like cumulonimbus).

Several methods have been proposed for conducting cloud classification on the satellite images. These can be grouped into three main categories: (1) Spectral-based (bi-spectral and split-window techniques); (2) Texture-based (texture analysis); and (3) Structure-based (spatial clustering), more information is given in [5,6]. Among these several techniques, the most popular ones are bi-spectral and split-window techniques. The bi-spectral approach identifies cloud types from their appearances invisible and thermal infrared images. Generally, clouds with cold tap (similar to cirrus or cumulonimbus) will appear brighter on thermal infrared images compared to the warmer low/middle clouds. Also, cirrus clouds usually appear dim in visual spectrum images but rather bright in thermal infrared images, while cumulonimbus appears bright in both images. Thick low/middle clouds with high albedo, such as cumulus clouds, appear bright in the visible spectrum but dim in the thermal infrared spectrum.

The split-window algorithm was initially proposed by Inoue [7] for automatic delineation of convective rainfall areas in the NOAA-TIR images and gaining widespread attention later on. In principle, it uses two equivalent brightness temperatures derived from two different IR bands; e.g., 10.5-11.5 μm (T_{11}) and 11.5-12.5 μm (T_{12}), from the weather satellites (like NOAA, MSG, GOES, or MTSAT) to identify potential cumulonimbus clouds on the image based on some chosen thresholds. The split-window technique is a simple but an effective method to identify cumulonimbus clouds in satellite images from their surrounding high clouds. This was initially proposed by Inoue [8] for automatic delineation of convective rainfall areas in the NOAA-TIR images and gaining widespread attention later on.

Researchers have developed a number of methods to detect clouds using satellite data. These methods include International Satellite Cloud Climatology Project [9], automated cloud screening of Advanced Very High Resolution Radiometer (AVHRR) [10]; Clouds detection from AVHRR (CLAVR-x) [11,12]; AVHRR Processing scheme Over cLoud, Land, and Ocean (APOLLO) [13];

and data from Meteosat Second Generation - Spinning Enhanced Visible and Infrared Imager MSG/SEVIRI cloud mask [14-16]; Cloud top height comparisons from Advanced Spaceborne Thermal Emission and Reflection Radiometer (ASTER), Multi-angle Imaging Spectro-Radiometer (MISR); Moderate-resolution Imaging Spectro-radiometer (MODIS) [17,18]; Cloud Detection with MODIS also improvements in the MODIS Cloud Mask for Collection [19]; Estimation of instantaneous net surface long wave radiation from MODIS cloud-free data [18,20]; Synergistic use of POLDER and MODIS for multi-layered cloud identification [21].

Nowadays, floods are the major disaster affecting many countries in the world year after year. It is an inevitable natural phenomenon occurring from time to time in all rivers and natural drainage systems, which not only damages the lives, natural resources, and environment, but also causes the loss of economy and health [22]. Rainfall intensity associated with each cloud type is an important parameter as it suggests the respective contribution of different categories of clouds to rainfall [23].

Clouds originate rain, which is very important in the daily lives of the world's population. The rainy clouds with high density are the main cause of flood event; detection and classification of clouds can be very effective for flood forecasting [24-27]. For this reason, the automated cloud detection of satellite imagery is important for understanding cloud temperatures and cloud classifications related to Thailand's rain-causing clouds.

2. The Study Area

The study area, which is shown in Figure 1, is located between latitudes 05° 37′ to 20° 27′N and longitudes 97° 22′E to 105° 37′E. Its area is 513,115.029 km^2. The climate is warm and tropical. Tropical monsoons and typhoons from both Andaman Sea and South China Sea contribute to the heavy rain in the region. The climates in Thailand now are as follows:

1. Rainy season usually starts when the southwest monsoon (from mid May onwards and stops mid-October)
2. From winter to mid-October until mid-February; and
3. Summer starting in mid-February to Mid-May.

The average annual rainfalls range from 1 000 to 1 500 mm for Northeastern and Central parts. But on the eastern tip and southern peninsula, the highest rainfalls average from 2 000 to 3 000 mm [28].

3. Materials and Methods

3.1 Data Collection

Satellite Imagery: The MTSAT-2 is a Japanese geostationary satellite with an operational period from 2010 to 2015. It has five spectral channels, which are in the following wavelength ranges: visible channel (0.55-0.90 μm), Thermal-Infrared channel IR1 (10.3-11.3 μm) and IR2 (11.5-12.5 μm), Water Vapor channel IR3 (6.5-7.0 μm), and Shortwave Infrared channel IR4 (3.5-4.0 μm).

The MTSAT-2 recorded data every hour (24 images per day). The spatial resolution of the visible image is about 1.00 km (nadir) and the Thermal-Infrared image is about 4.00 km (nadir). The MTSAT-2 data were acquired from the website: http://www.jma.go.jp/jma/jma-eng/satellite/index.html [29].

The sample data of the satellite in visible channel are shown in Figure 2.

3.2 Development SML and EML Script Language

The ERDAS Imagine is commercial software for geospatial applications [30]. The ERDAS Developers'

Figure 1: Thailand boundary.

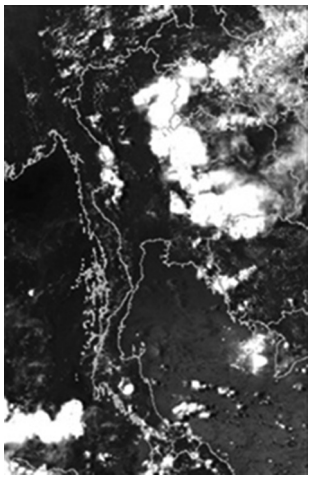

Figure 2: Sample MTSAT-2 data in visible channel.

toolkit uses the C or C++ programming language and comprises application programming interfaces (APIs) to be modified for the user's specific needs [31]. ERDAS Imagine includes a graphical user interface (GUI) scripting language known as the ERDAS Macro Language (EML). The capabilities of EML are extensive for the needs of both users and programmers. Using these capabilities, the author was developed platform of GUI from EML to ease the burden of formatting data and entering switches on a command line. In addition, ERDAS Imagine includes a modeling language, known as Spatial Modeler Language (SML), which uses a graphical editor for creating models. Consequently, this platform developed is helpful to save the time of basic input and output interface design and batch processing. The platform developed was created for use by MTSAT-2 data where the available conversion look-up table was an extended utility platform design in ERDAS Imagine menu. The GUI interface of this integrated platform is added to ERDAS Imagine as shown in Figure 3.

Figures 4 and 5 illustrate sample of programming by using SML and EML script language.

3.3 Development of a Cloud Classification Model

This research focuses on analyzing cloud distributing patterns over the entire coverage area. The used rainfall data were referred earlier and the corresponding cloud top temperature maps were derived from the developed model. In brief, the main steps in establishing of this cloud classification model are as follows:

Radiance to brightness temperature conversion: The cloud top temperature could be generated directly by applying the standard look-up table. The conversion table has been formulated anchored in Planck's constant function and sensor's spectral response functions from which the approximated conversion formula is specified as follows [24].

$$B_i(T_b) = 2hc^2V_i^3/exp\{hcv_i/k(a_{1i} + a_{2i}T_b) - 1\} \quad (1)$$

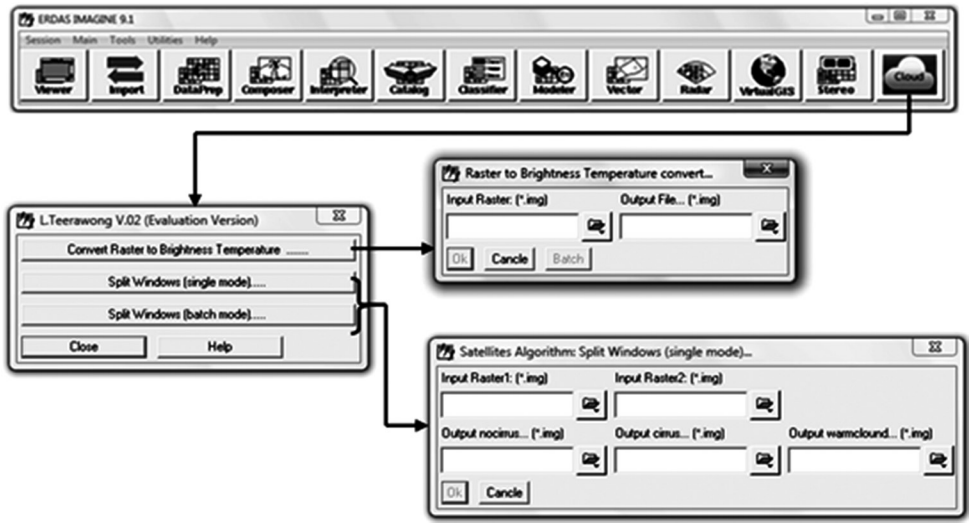

Figure 3: Extended utility platform design and development.

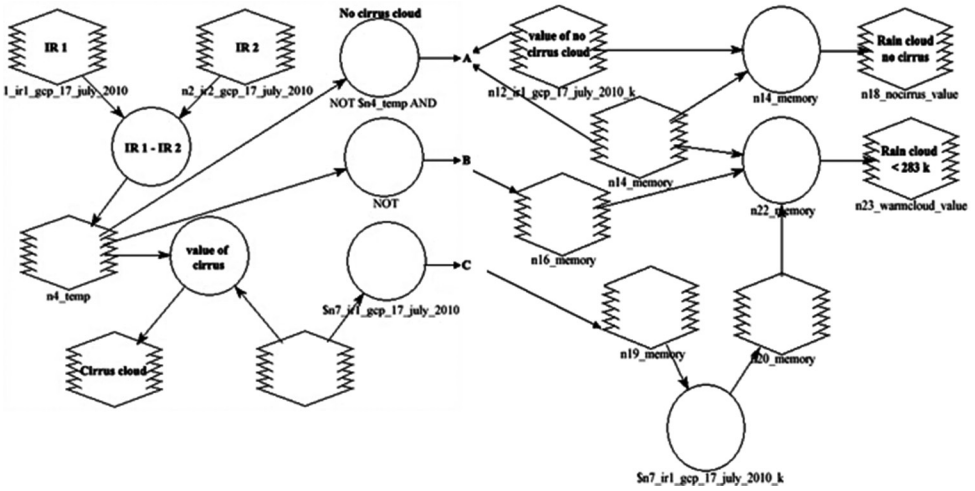

Figure 4: Illustrate sample programming by using EML script.

Where, B_i is the Planck function (or observed radiance) of sensor's channel i; T_b is the BT; ν_i is central wave number of channel i; a_{1i} and a_{2i} are band correction coefficients of channel i; h and k are Planck and Boltzmann constants respectively; and c is the speed of light in vacuum.

The value constants a_1 and a_2 for each MTSAT-2 data are given in Table 1. In this context, brightness temperature is the equivalent temperature at the surface of objects, e.g., clouds, under observation from which the measured radiance was first released.

The brightness temperature threshold was set at 10°C in cloud cover image. Thus, most of the background objects on the Earth's surface as well as some warm clouds having the cloud top temperature greater than 10°C were screened off. In addition, it enables the warm clouds with cloud top temperature between 0 and 10°C and the mixed cold cloud and warm cloud that may have temperature between 0 and −20°C detectable. The detection ion of cloud types on the images was still not performed at this stage, but generally, the clouds with temperature 10 to −20°C are growing cumulus or some stratiform clouds that might be able to produce a shower or light rainfall, not the heavy one. Nevertheless, the clouds with temperature less than −40 or −50°C are likely to be the cumulonimbus which can possibly be cold-high clouds such as the cirrus also. In this work, the brightness temperature data on the cloud images were classified into eight classes (at 10°C interval) as described in Table 2.

```
#*********************************************
COMMENT "Author: Teerawong Laosuwan";
COMMENT " Program name: IR1 Convert to temperature.mdl";
COMMENT "Generated model: IR1 Convert to temperature";
#*********************************************
#
# set cell size for the model
#
SET CELLSIZE MIN;
#
# set window for the model
#
SET WINDOW UNION;
#
# set area of interest for the model
#
SET AOI NONE;
#
# declarations
#
Integer RASTER n1_mt1r06030600 FILE OLD NEAREST NEIGHBOR
AOI NONE arg1;
Float RASTER n3_out FILE DELETE_IF_EXISTING IGNORE 0
ATHEMATIC
 FLOAT DOUBLE arg2;
#
# function definitions
#
n3_out = CONDITIONAL {
($n1_mt1r06030600==0) 329.941500,
($n1_mt1r06030600==1) 329.625500,
($n1_mt1r06030600==2) 329.309500,
($n1_mt1r06030600==3) 328.993500,
        ▼
    QUIT;
```

Figure 5: Illustrate sample programming by using SML script.

4. Result

This study summarizes the effectiveness of using this software platform to detect and classify clouds over the coverage area. In detail, graphic user interface design with EML, main modules and relative functions, and module development of this platform are introduced in detail. This designed platform has advantages of integrating multi-functions in ERDAS Imagine software, and separating the manual work and artificial automated operation. According to process and analysis, this platform enhances man-machine interaction capability and improves the change detection efficiency, which can provide a reference to application of secondary development based on existing remote sensing professional software. The sample of radiance brightness temperature conversion from MTSAT-2 image is shown in Figure 6.

Cloud type classification: The innovative cloud classification model developer is to classify the types of clouds that appeared in the satellite data (in the form of the cloud top temperature maps). The MTSAT-2 data from band 1 (IR1 or T_{11}) and 2 (IR2 or T_{12}) were selected for using in the split-window analysis.

High cloud filtering: The calculation was performed for ΔT (T_{11}–T_{12}) [32]; from the data, high cloud filtering thresholds are $T_{11} < 253$ K(−20°C) and $\Delta T > 1$ K. The applications of these thresholds are shown in Table 3.

Table 1: The values constants of MTSAT-2

Channel	Wave number ν (cm^{-1})	Channel correction coefficients	
		a_1	a_2
IR1 (10.8 μm)	926.4627	0.3597851	0.9987568
IR2 (12.0 μm)	835.6672	0.2195110	0.9991676
IR3 (6.80 μm)	1476.6898	0.3645235	0.9991492
IR4 (3.80 μm)	2684.1181	2.4635230	0.9967825

Table 2: Illustration cloud top temperature classification

Class	Range (In °C)	Range (In K)	Potential cloud types
1	0 to 10	273 to 283	Warm cloud
2	−10 to 0	263 to 273	Like cumulus or stratus
3	−20 to −10	253 to 263	Mixed clouds
4	−30 to −20	243 to 253	
5	−40 to −30	233 to 243	
6	−50 to −40	223 to 233	Cumulonimbus or cold high clouds
7	−60 to −50	213 to 223	
8	<−60	<213	

Cloud classification: Three steps were developed to completing this objective: (1) input MTSAT-2 image files channel IR1 and IR2, (2) filtering high clouds on the input data as given thresholds that are primarily set in the script (T_{11} and $\Delta T = T_{11} - T_{12}$), and (3) the output cloud map files which are cirrus mapped, cirrus filtered map, and all classified typical cloud based on the Earth's surface temperature standard as 283 K (10°C) [33].

Cloud distribution data from July 29, 2010 were used in this analysis. On that date, the cold air mass (weather front) was weakened and gave a chance to the warm moist air streams from the Gulf of Thailand to move into the central and lower northeastern region.

a. Histogram in brightness values and
b. Histogram in brightness temperature (Kelvin).

This results in the formation of cloud (rain cloud) along the weather front and by local convective process. Most of the cold clouds were developed during the daytime and normally only lasted just a few hours. But the long-lasting cold cloud was seen at nighttime in the central area, where it could be visible for more than 10 hours. Mainly potential warm clouds at temperature 10 to –10°C were seen in the afternoon but some can last all night long. The hourly amount of the cloud cover (hourly 1 – hourly with Coordinated Universal Time on July 29, 2010) at each temperature range is shown in Figures 7-9. The high cloud filtering calculation was performed for $\Delta T = T_{11} - T_{12}$, as shown in Figure 10.

Table 3: Brightness temperature and ΔT for high cloud and cumulonimbus cloud

Cloud type	Parameter	Mean	Minimum	Maximum	SD
High clouds	IR1 (11μm)	253.72	222.45	284.83	14.03
	IR2 (12μm)	249.89	219.48	280.44	13.03
	ΔT	3.83	2.97	4.39	1.00
Cumu lonimbus	IR1 (11μm)	233.83	197.61	284.82	28.24
	IR2 (12μm)	231.39	198.09	280.43	26.18
	ΔT	2.39	–0.48	4.39	2.09

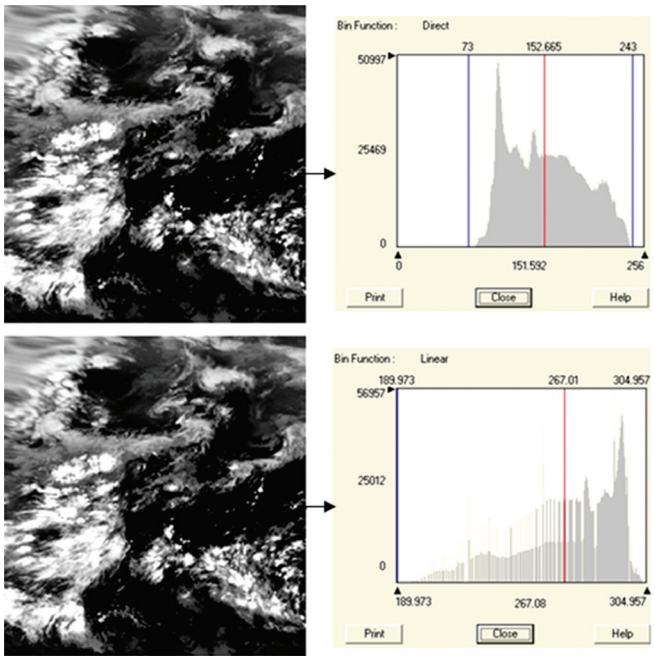

Figure 6: Sample radiance brightness temperature conversions.

5. Conclusion

Automated cloud detection of the satellite imagery using SML and EML was used to distinguish between cold high clouds. The potential high clouds were filtered at the beginning of the classifying process using split-window method in which the threshold temperatures $T_{11} < 253$ K (–20°C) and $\Delta T > 1$ K ($T_{11} - T_{12}$) were employed according to values being analyzed from cloud samples. The cloud top temperature was then generated and all clouds with cloud top temperatures more than 10°C were identified on maps and used to describe patterns of cloud distribution. In this study, software select reasons of the integrated platform are summarized and the cloud detection and classification work flow is presented. The interface design's use of SML and EML are described in detail. In addition, our automated cloud detection classification system was built within the working environment

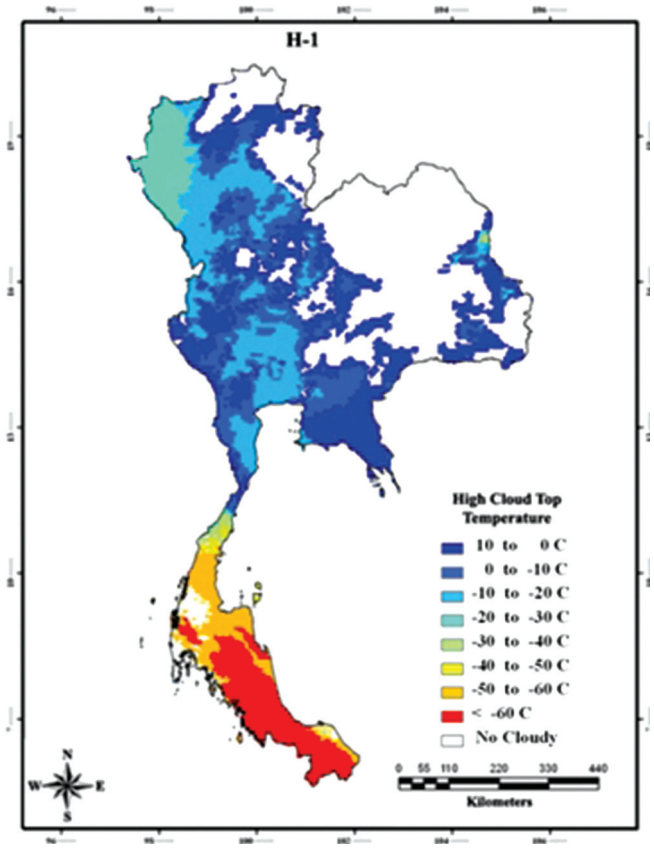

Figure 7: High cloud top temperatures (Hourly 1).

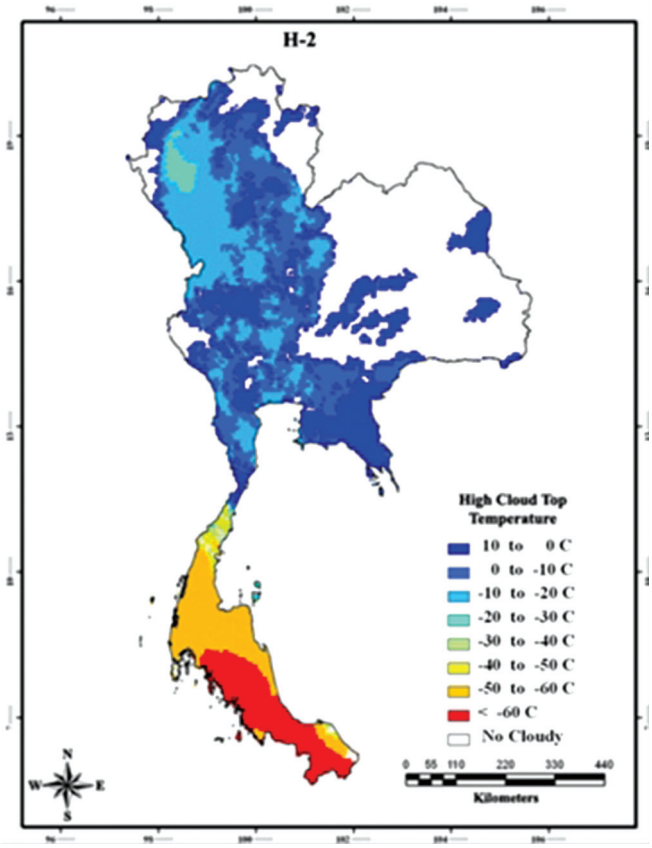

Figure 8: High cloud top temperatures (Hourly 2).

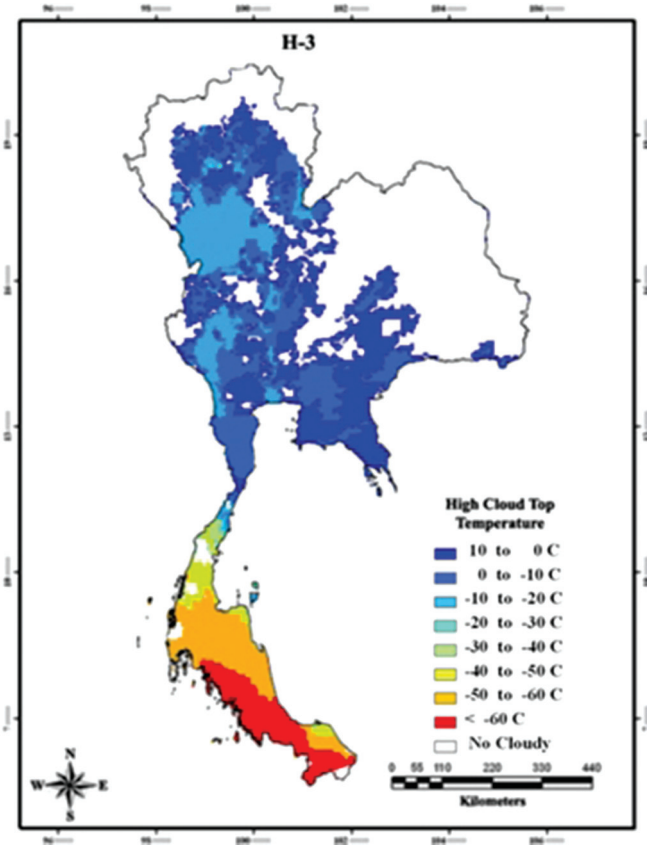

Figure 9: High cloud top temperatures (Hourly 3).

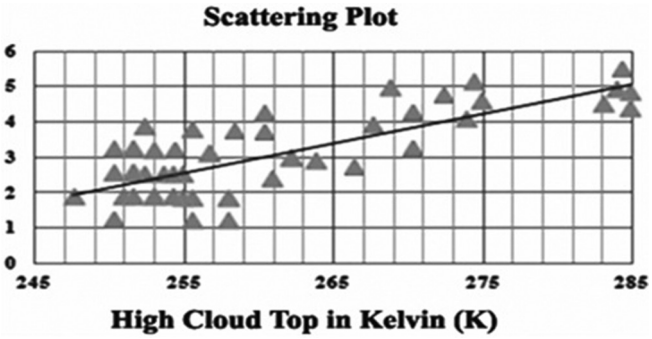

Figure 10: Brightness temperature and ΔT scattering.

provided by the commercial remote sensing software, ERDAS Imagine.

Satellite rainfall estimation is important for monitoring, warning, and mitigation of rain disasters such as flash flood which becomes more and more serious nowadays. However, dynamic rain processes are different from region to region due to geographical and climatic differences and other relevant factors; rainfall estimation technique suitable for global coverage does not exist. However, the relationship between satellite data from each type of sensors and rain rate collected from rain gauges in regions of interest must be investigated.

In this research, the author proposed an automated cloud detection of satellite imagery using Spatial Modeler Language and ERDAS Macro Language. The rain rate depends on other relevant factors such as geographical areas and climatic region, especially rain synoptic in the region of interest which must be further studied in the future.

6. Acknowledgment

The author would like to thank Prof. Dr. Paisan Laosuwan, Dean, Faculty of Science and Technology, Hatyai University for his guidance and feedback throughout the development of the research. The author also would like to thank Dr. Porntip Bumrungkang, MD, Paragon InfoTech (Thailand) Co., Ltd for her advice and support in during of this study.

References

1. V. Laine, and A. Venalainen, "Estimation of surface solar global radiation from NOAA AVHRR data in high latitudes," Journal of Applied Meteorology, Vol. 38, pp. 1706-19, 1999.
2. J.M. Yeom, K.S. Han, Y.S. Kim, and J.D. Jang, "Neural network determination of cloud attenuation to estimate insolation using MTSAT-1R data," International Journal of Remote Sensing, Vol. 29, pp. 6193-208, 2008.
3. R.P. Allan, "Combining satellite data and models to estimate cloud radiative effect at the surface and in the atmosphere," Meteorological Applications, Vol. 18, pp. 324-33, 2011.

4. A.K. Tripathi, and S. Mukhopadhyay, "Removal of fog from images: A review," IETE Technical Review, Vol. 29, no. 2, pp. 148-56, 2012.
5. R. Kaur, and A. Ganju, "Cloud classification in NOAA AVHRR imageries using spectral and textural features," Journal- Indian Society of Remote Sensing, Vol. 36, pp. 167-74, 2008.
6. H.U. Yong, Z. Chun-xia, and W. Hong-nan, "Automatic Pavement Crack Detection Using Texture and Shape Descriptors," IETE Technical Review, Vol. 27, no. 5, pp. 398-405, 2010.
7. T. Inoue, "On the Temperature and Effective Emissivity Determination of Semitransparent Cirrus Clouds by Bispectral Measurements in the 10 μm Window Region," Journal of Meteorology Society Japan, Vol. 63, pp. 88-98,1985.
8. T. Inoue, "A Cloud Type Classification with NOAA 7 Split-Window Measurements," Journal of Geophysical Research. Vol. 92, pp. 3991-4000, 1987.
9. W.B. Rossow, and L.C. Garder, "Cloud Detection Using Satellite Measurements of Infrared and Visible Radiances for ISCCP," Journal of Climate, Vol. 6, pp. 2341-69, 1993.
10. T.C. Gallaudet, and J.J. Simpson, "Automated cloud screening of AVHRR imagery using split-and-merge clustering," Remote Sensing of Environment, Vol. 38, pp. 77-121, 1991.
11. L.L. Stowe, P.A. Davis, and E.P. McClain, "Scientific Basis and Initial Evaluation of the CLAVR-1 Global Clear/Cloud Classification Algorithm for the Advanced Very High Resolution Radiometer," Journal of Atmospheric and Oceanic Technology, Vol. 16, pp. 656-81, 1999.
12. K.T. Kriebel, G. Gesell, M. Ka¨stner, and H. Mannstein, "The cloud analysis tool APOLLO: Improvements and validations," International Journal of Remote Sensing, Vol. 24, pp. 2389-408, 2003.
13. M. Derrien, and H. Le Gléau, "MSG/SEVIRI cloud mask and type from SAFNWC," International Journal of Remote Sensing, Vol. 26, pp. 4707-32, 2005.
14. F. Porcù, M. Borga, and F. Prodi, "Rainfall estimation by combining radar and infrared satellite data for now casting purposes," Meteorological Applications, Vol. 6, pp. 289-300, 1999.
15. I. Genkova, G. Seiz, P. Zuidema, G. Zhao, and L. Di Girolamo, "Cloud top height comparisons from ASTER, MISR, and MODIS for trade wind cumuli," Remote Sensing of Environment, Vol. 107, pp. 211-22, 2007.
16. A. Behrangi, H. Kuo-lin, B. Imam, S. Sorooshian, and R. J. Kuligowski, "Evaluating the Utility of Multispectral Information in Delineating the Areal Extent of Precipitation," Journal of Hydrometeorology, Vol. 10, pp. 684-700, 2009.
17. S.A. Ackerman, K.I. Strabala, W.P. Menzel, R.A. Frey, C.C. Moeller, and L.E. Gumley, "Discriminating clear sky from clouds with MODIS," Journal of Geophysical Research: Atmospheres, Vol. 103, pp. 32141-57, 1998.
18. R.A. Frey, S.A. Ackerman, Y. Liu, K.I. Strabala, H. Zhang, and J.R. Key, *et al*., "Cloud Detection with MODIS. Part I: Improvements in the MODIS Cloud Mask for Collection 5," Journal of Atmospheric and Oceanic Technology, Vol. 25, pp. 1057-72, 2008.
19. B. Tang, and Z.L. Li, "Estimation of instantaneous net surface longwave radiation from MODIS cloud-free data," Remote Sensing of Environment, Vol. 112, pp. 3482-92, 2008.
20. Z. Yao, Z. Han, Z. Zhao, L. Lin, and X. Fan, "Synergetic use of POLDER and MODIS for multilayered cloud identification," Remote Sensing of Environment, Vol. 114, pp. 1910-23, 2010.
21. D. Fraser, R.A. Massom, and K.J. Michael, "Generation of high-resolution East Antarctic landfast sea-ice maps from cloud-free MODIS satellite composite imagery," Remote Sensing of Environment, Vol. 114, pp. 2888-96, 2010.
22. L. Teerawong, and N.K. Tripathi, "Potentiality of data fusion techniques for flood identification," Proc. of USPAM Conference, Hanoi, Vietnam. 6-8 Mar. 2007.
23. J.K. Mishra, and O.P. Sharma, "Cloud top temperature based precipitation intensity estimation using INSAT-1D data," International Journal of Remote Sensing, Vol. 22, pp. 969-85, 2001.
24. H. Azari, A.A. Matkan, A. Shakiba, and H. Pourali, "Classification of clouds with object oriented technique," ISPRS TC VII Symposium 100 Years ISPRS-Advancing Remote Sensing Science, Vienna, Austria, 5-7 Jul. 2010.
25. A. Manjunath, D. Jain, S. Kumar, and R. Anjaneyulu, "Role of Satellite Communication and Remote Sensing in Rural Development," IETE Technical Review, Vol. 24, no 4, pp. 215-24, 2007.
26. S. Inamdar, and S. Chaudhuri, "Temporally Adaptive, Partially Unsupervised Classifiers for Remote Sensing Images," IETE Technical Review, Vol. 24, no 4, pp. 249-56, 2007.
27. U. Mangai, S. Samanta, S. Das, and P. Chowdhury, "A Survey of Decision Fusion and Feature Fusion Strategies for Pattern Classification," IETE Technical Review, Vol. 27, no 4, pp. 293-307, 2010.
28. Thai Meteorological Department, "The average annual rainfalls in Thailand." Available from: http://www.tmd.go.th [Last accessed on 2011 Jan 18].
29. Meteorological Satellite Center, "MTSAT-2 data." Available from: http://mscweb.kishou. go.jp/index.htm [Last accessed on 2010 July 20].
30. Leica Geosystems, ERDAS IMAGINE Configuration Guide for Windows, GIS and Mapping, LLC Atlanta, Georgia, 2003.
31. Leica Geosystems, ERDAS Macro Language Reference Manual, ERDAS, Inc. Atlanta, Georgia, 2000.
32. T. Inoue, M. Satoh, H. Miura, and B. Mapes, "Characteristics of Cloud Size of Deep Convection Simulated by a Global Cloud Resolving Model over the Western Tropical Pacific," Journal of the Meteorological Society of Japan. Ser. II, Vol. 86A, pp. 1-15, 2008.
33. Climate and Weather Systems, "Lecture 1: Light and Energy in the Atmosphere." Available from: http://www.st-andrews.ac.uk/~dib2/climate/energy.html [Last accessed on 2011 October 02].

AUTHORS

Teerawong Laosuwan received his B. Ind. Tech (Electronics Engineering) from South East Asia University, Thailand in 1996, M.Sc. (Remote Sensing) from Suranaree University of Technology, Thailand, in 2001. He obtained certificate of Geoinformatics and GIS Modeling from ITC, University of Twente, Netherlands in 2005 and CAS (Remote Sensing and GIS) from Asian Institute of Technology (AIT), Thailand in 2010. His scientific publications such as Urban Heat Island Monitoring and Analysis by Using Integration of Satellite Data and Knowledge Based Method, Improving Satellite Remote Sensing in Multi Spectral through Image Fusion Algorithm, and An Innovative Approach to the Development of Spatial Data Infrastructures and Web 2.0 Technologies.

E-mail: teerawong@msu.ac.th

Singthong Pattanasethanon received his Ph.D. (Energy Technology) from Mahasarakham University, Thailand. Presently, he is with the lecturer and researcher in the Department of Electrical and Computer Engineering, Faculty of Engineering, Mahasarakham University. His scientific publications such as Empirical modeling and the forecasting illuminance/irradiance on horizontal plane using artificial neural network for all sky types at Mahasarakham, Thailand, Sky modeling daylight availability and illuminance/irradiance on horizontal plane for Mahasarakham, Thailand, and An Availability of Sky Luminance in Tropical Climate to Standard Voltages Conversion by Using Artificial Neural Network.

E-mail: singthong.p@msu.ac.th

Worawat Sa-ngiamvibool received his B. Eng. and M. Eng. in Electrical Engineering, Khonkaen University, Thailand, and his Ph.D. in Electrical Engineering, SIIT, Thammasat University, Thailand. His main research of interest includes Analogue Circuit, Optimization Technique and Technology Management. Presently, he is lecturer and researcher in the Department of Electrical and Computer Engineering, Faculty of Engineering, Mahasarakham University. His scientific publications include Identification of Shear Band using Elastic Shear Wave Propagation, Identification of Shear Band using Elastic Shear Wave Propagation, and A 10.7-MHz Fully Balanced, High-Q, 87-dB-Dynamic-Range Current-Tunable Gm-C Bandpass Filter.

E-mail: wor_nui@yahoo.com

DOI: 10.4103/0256-4602.113486; Paper No. TR 694_12;